

Impact of ADC Sampling Rate and Number of Bits on the Matched Filter Efficiency in Intrapulse LFM Radar

André Krüger, Derek Nogueira, Renato Machado, Dimas Irion Alves, and Olympio Coutinho

Abstract – This paper analyzes the effects of changing the sample rate and the number of bits of a linearly frequency-modulated (LFM) pulse on a matched filter-based radar detector. For this purpose, a radar simulator with close to real parameters is used. Changes in the values of those variables are made separately and in combination, verifying their impacts. A reduction of the average sidelobe power and the compression gain was observed with an increase in the number of bits, stabilizing after the fourth bit. Regarding the sampling rate changes, the compression gain was not altered by its variation, unlike the sidelobe power.

Keywords – *Quantization, compression gain, sidelobe level.*

I. INTRODUCTION

Modern radars commonly employ pulse compression techniques to improve the signal-to-noise ratio (SNR) of the received signal [1]. This technique transmits a signal with intrapulse modulation and a known coding. The transmitted pulse has characteristics of long duration, low amplitude, and, consequently, low power, intending to have a high transmitted energy [2]. A widely used encoding is the linear intrapulse frequency modulation. Once in the receiver, the pulse is injected into a matched filter that, from the knowledge of the modulation code of the transmitted pulse, performs energy compression in time. This dramatically concentrates all the energy transmitted in one long pulse into a short interval [2]. This power compression produces an increase in the amplitude of the received signal. Thus, a significant improvement in SNR is obtained, considering that the noise present in the signal does not have the same modulation code matched to the filter.

A current trend in the development of radar systems is the use of digital signal processing. Indeed, the best conditions of the number of bits and sampling rate are sought to maintain the fidelity of the desired signal compared to the analog one. This scenario suggests increasing the number of bits and sampling rate. On the other hand, considerations of cost, power consumption, system size, and complexity suggest reducing this sample rate and number of bits as much as possible. Then, analyzing the pulse compression efficiency against the number of bits and sample rate can help optimize these two important parameters of the digital signal processor.

An analysis of the effects of the number of bits in an LFM signal after the matched filter has been done by [3]–[6]. Specifically, in [3], such an analysis was conducted on a signal generated by a digital radio frequency memory (DRFM) and found an increase in the level of the sidelobes when reducing the number of bits. On the other hand, [4] and [5] performed simulations of injecting an LFM signal directly into a matched filter. Both obtained a reduction of the average sidelobe power up to a certain number of bits. Although the focus in [6] is on

mismatched pulse compression filters, the results of the sidelobe were similar to those obtained by other authors. Finally, regarding the sampling rate, according to the analysis presented in [7], it was found that the signal energy does not change with the modification of that parameter.

However, no study has attempted to perform a cross-analysis of these variables. Thus, this paper initially presents a comparative analysis considering each parameter individually. Then, a study combining both variables and verifying their effects on the signal after the matched filter is performed. The results obtained in the individual analysis are close to those obtained by other authors. With an increase in the number of bits, the sidelobe power, as well as the compression gain, tends to decrease. With an increase in the sampling rate, the compression gain does not change, but the sidelobe level does. This makes that different combinations of these parameters deliver the same results.

This paper is organized as follows. Section II discusses a theory of the matched filter and some particularities. Section III comments on the methodology of the simulations performed in this work. Section IV discusses the results obtained, ending with Section V, with a brief conclusion.

II. MATCHED FILTER

In radar detection, the higher signal-to-noise ratio (SNR), the greater target detection distance. Several factors influence the SNR, such as radar operating power, the gain of its antennas, target radar cross section (RCS), noise, and general losses [1]. However, even operating under better conditions of these parameters, some characteristics are beyond the radar operator's management, such as thermal noise. Always present in electronic systems, there must be a way to circumvent the negative influence of this factor. One way widely used is through the filters that maximize the SNR through pulse compression in time [1].

Considering the continuous-time analysis, the output signal of a matched filter at a time instant T_M can be expressed as [2]:

$$|y(T_M)|^2 = \left| \frac{1}{2\pi} \int_{-\infty}^{\infty} X(\Omega)H(\Omega)e^{j\Omega T_M} d\Omega \right|^2, \quad (1)$$

where $X(\Omega)$ is the frequency spectrum of the transmitted radar signal waveform, and $H(\Omega)$ is the frequency response of the filter in question.

On the other hand, the total white noise power at the filter output is given by [2]:

$$n_p = \frac{\sigma_w^2}{2\pi} \int_{-\infty}^{\infty} |H(\Omega)|^2 d\Omega, \quad (2)$$

where σ_w^2 is the spectral density of the white noise power at the output of the filtering process. Thus, the maximum signal-to-noise ratio obtained at the time instant T_M is given by:

$$\text{SNR} = \frac{|y(T_M)|^2}{n_p} = \frac{\left| \frac{1}{2\pi} \int_{-\infty}^{\infty} X(\Omega) H(\Omega) e^{j\Omega T_M} d\Omega \right|^2}{\frac{\sigma_w^2}{2\pi} \int_{-\infty}^{\infty} |H(\Omega)|^2 d\Omega}. \quad (3)$$

Observing (3), one can infer that the SNR is directly related to the product of the filter frequency response and the radar signal spectrum. To better define it, a parallel is made with the Cauchy-Schwarz inequality, defined by [8]:

$$\left| \int_{-\infty}^{\infty} P(x) Q(x) dx \right|^2 \leq \int_{-\infty}^{\infty} |P(x)|^2 dx \int_{-\infty}^{\infty} |Q(x)|^2 dx. \quad (4)$$

Substituting the inequality (4) in (3), thus:

$$\text{SNR} \leq \frac{(1/2\pi)^2 \int_{-\infty}^{\infty} |X(\Omega) e^{j\Omega T_M}|^2 d\Omega \int_{-\infty}^{\infty} |H(\Omega)|^2 d\Omega}{(\sigma_w^2/2\pi) \int_{-\infty}^{\infty} |H(\Omega)|^2 d\Omega}. \quad (5)$$

The maximum signal-to-noise ratio occurs at an instant of time T_M , where:

$$H(\Omega) = X^*(\Omega) e^{-j\Omega T_M}, \quad (6)$$

which is the complex conjugate of the generated waveform. This is the transfer function of the ideal matched filter, which can be seen as a filter designed for a specific waveform that optimizes the SNR when the received signal is contaminated only by an additive white Gaussian noise.

One particularity of a radar receiver that uses a matched filter is the output SNR of the signal. It depends only on the total energy of the received pulse, defined by its amplitude and duration, and on the pulse bandwidth, which defines the noise power. Then, the SNR can be re-written as [9]:

$$\text{SNR} = \frac{1}{2\pi\sigma_w^2} \int_{-\infty}^{\infty} |X(\Omega)|^2 d\Omega. \quad (7)$$

Applying Parseval's theorem to determine the energy of the pulse, we obtain:

$$\text{Energy} = \int_{-\infty}^{\infty} |x(t)|^2 dt = \frac{1}{2\pi} \int_{-\infty}^{\infty} |X(\Omega)|^2 d\Omega. \quad (8)$$

Finally, the SNR can be expressed by

$$\text{SNR} = \frac{\text{Energy}}{\sigma_w^2}. \quad (9)$$

It is possible to observe that the above analyses were performed in continuous time. However, they are still valid for discrete signal processing, as in the simulations presented in this paper [1].

III. SIMULATION METHODOLOGY AND MODELING

The simulations performed in this paper were done using Matlab software and are based on the model proposed by Moura [10] whose simplified architecture can be seen in Fig. 1. In his work, a simulator of a surveillance radar was made with parameters similar to those used in real systems. We decided to use it as a base to have results close to those found in real-world scenarios and not only unattainable theoretical values. The values used in the simulator are shown in Table I.

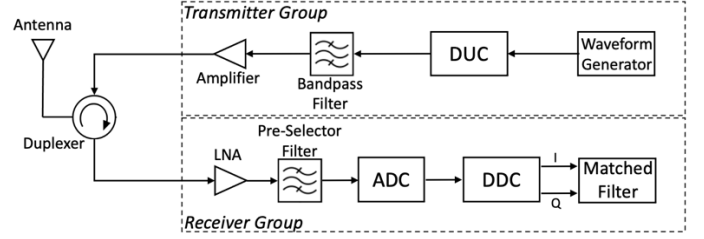


Fig. 1 – Simplified simulation architecture.

Table I – Radar parameters

Parameters	Value
Peak power	40 kW
Pulsewidth	300 μ s
Bandwidth	600 kHz
Carrier frequency	1237.5 MHz
Noise figure	1.8 dB
Maximum antenna gain	37 dB
Transmission losses	1.5 dB

The model in Fig. 1 starts with the generation of a LFM waveform and initial phase $\phi_i = \pi$. Its complex representation in the discrete time domain is given by

$$x[t] = \text{rect}\left(\frac{t-\tau/2}{\tau}\right) e^{j\pi\frac{B_w}{\tau}(t-\tau/2)^2 + j\phi_i}, \quad (10)$$

where τ is the pulsewidth and B_w the bandwidth.

In the next steps, the signal $x[t]$ goes through a digital up converter (DUC). Then, it passes through a bandpass filter, an amplification process related to the transmit antenna gain, radar peak power, and system losses to be radiated.

As the objective of this work is to analyze the effects of the number of bits and a sampling rate of a pulse in the matched filter to avoid any form of external interference in the results, the propagation of the pulse and its reflection on the target were disregarded. In this way, immediately after being transmitted, the pulse is already received, amplified, and mixed with white noise, obtaining the contaminated signal $x'[t]$. The next steps of its passage through the pre-selector filters, analog-to-digital converter (ADC), digital down conversion (DDC), and the other steps of a radar receiver are well described in [10].

Specifically about the insertion of quantization noise into the signal $x'[t]$, we modeled a uniform midrise transfer function (TF) of an ADC as described in [11]. The TF can be represented with 2^b elements differentiated from each other by one LSB (Least Significant Bit based on the ADC's full scale), where b is the number of bits tested.

$$TF = [(-LSB)2^{b-1} \dots (+LSB)2^{b-1}]. \quad (11)$$

Then, each $x'[t]$ sample passes through the linear quantization process, generating the quantized signal $x'_q[t]$. As an example, the result for an 8-bit ADC is shown in Fig. 2.

It should be noted that nonlinearity and offset errors in the ADC transfer function have been disregarded. Thus, the SNR due to the quantization process can be estimated by [12]:

$$\text{SNR(dB)} = 6,02^b + 1,76. \quad (12)$$

Therefore, the theoretical values for an ADC with 4 and 8 bits are 25.84 dB and 49.92 dB. The values measured in this modeling for the same number of bits were 25.56 dB and 49.21 dB, a fact that validates this transfer function. The small perceived difference is related to the choice of a scale background slightly larger than the peak of the signal $x'[t]$ to avoid possible clipping of the input signal.

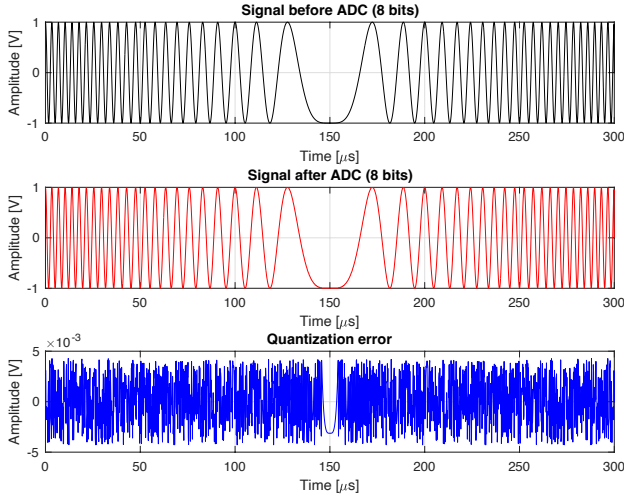


Fig. 2 – Inserting the quantization error in the signal $x'[t]$.

After passing through the ADC, the signal $x'_q[t]$ arrives at the matched filter. The impulse response $h[t]$ of the filter in question was designed according to the waveform $x[t]$, as defined in (6). It is emphasized that once the sampling rate of the signal is chosen, it is the same as $h[t]$ and remains constant at all stages of the radar processing.

Finally, based on (1), the convolution process is performed between the input signal and the impulse response $h[t]$ of the matched filter. To reduce computational processing, this step was performed in the frequency domain by using the fast Fourier transform (FFT) and its inverse transform (IFFT), as described below:

$$y[t] = IFFT \{ FFT \{ x'_q[t] \} FFT \{ h[n] \} \}. \quad (13)$$

IV. RESULTS

Simulations were run to analyze the effects of the ADC number of bits and the sampling rate in a signal after the matched filter. At the end of these simulations, the results obtained were stored and compared with each other in order to check their constancy and robustness. The difference found in the values of the results at each run occurred only at a centesimal level, caused by the behavior of the existing white noise.

Initially, only the number of bits was varied, from 1 to 8, and all other characteristics were kept constant. Later, for a fixed number of bits, the sampling rate was modified between 640 kHz, 6.7% higher than the minimum frequency stipulated by the Nyquist criterion, and up to 10 times this value. Finally, simulation rounds were performed in which both variables were changed together.

A. Quantization Effects

In this simulation round, the sampling rate was fixed at 640 kHz by varying only the number of bits. In Fig. 3, it is possible to see the signal in the time domain after the matched filter. It can be seen that the increase in the number of bits has a direct effect on the behavior of the sidelobes. This result agrees with the results obtained by [3], [4] e [6].

Specifically in [3], the decrease in the number of bits generated a more prominent increase in the average power of the right side lobe of the signal, a fact not observed in the results of this work. The explanation for this difference is supported by the scenario simulated in that paper since it deals with the bit variation of a DRFM in a radar interference process. The tendency of the behavior of both sidelobes was the same, except for some details caused by the differentiation in the experiments.

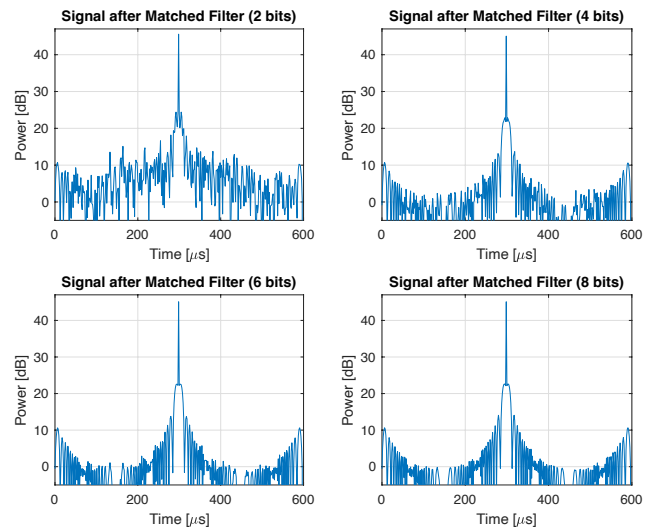


Fig. 3 – Matched filter output for different bit values.

The signal compression gain and the average sidelobe power were measured for each scenario and are presented in Fig. 4.

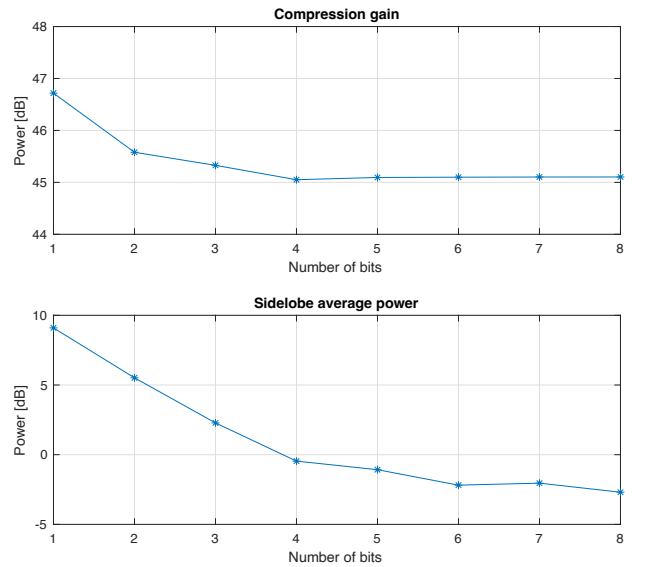


Fig. 4 – Analysis of compression gain (main lobe) and average side lobe power.

When analyzing the effect of the increment in the number of bits on the compression gain, it can be seen that there is a

slight decrease in power up to 4 bits stabilizing after this value. This trend was also observed in [5]. Finally, the average power of the sidelobes also showed similar behavior of falling sharply up to 4 bits, as also evidenced by [3] and [4].

Such a tendency is justified in the quantization process. An analog signal passing through a 1-bit ADC has its samples rounded to LSB-based values. Sometimes these roundings are to absolute values larger than those observed in the analog signal (as shown in Fig. 5). With a larger number of bits, this effect is minimized to the point that it doesn't make a significant difference when the number of bits increases.

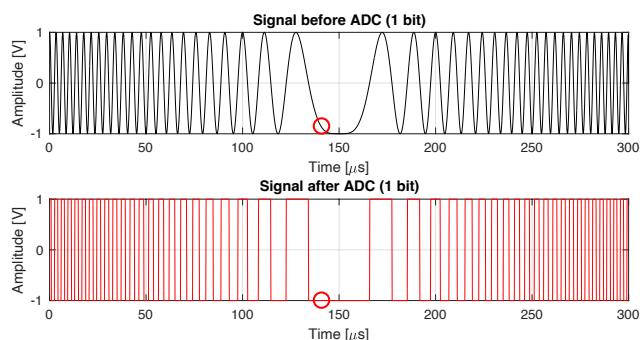


Fig. 5 – Effect of the quantization error. Simulation with 1 bit.

Another way to analyze this effect occurs in the frequency domain. Performing the Fourier Transform of the same signal mentioned above and of a signal with 8 bits, we obtain the power spectra of Fig. 6. It can be seen that, due to the explanation commented earlier, the power of the 1-bit quantized signal is higher than that of the 8-bit signal in almost every range of the analyzed spectrum.

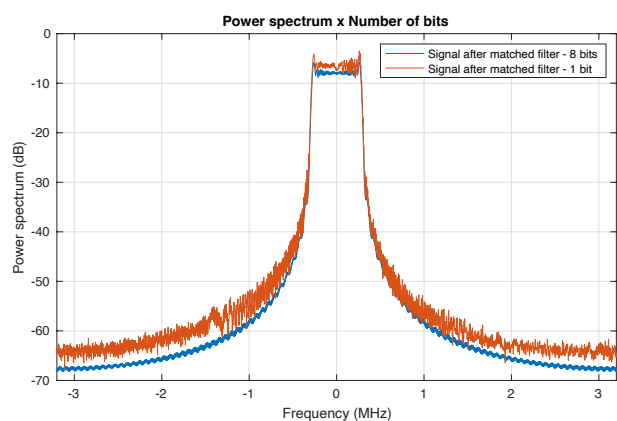


Fig. 6 – Comparison of power spectra after the matched filter.

B. Sampling Rate Effects

In this round of experiments, the number of bits was fixed at 8 and only the sampling rate of the signal was varied from one to four times the minimum frequency stipulated by the Nyquist criterion (640 kHz), as shown in Fig. 7. Even though 6.7% above the theoretical one for this complex signal, it was used due to the imperfections existing in real filters.

It is possible to see the effect of the increased sampling rate on the behavior of the sidelobes. More influential at frequencies near the theoretical minimum threshold, the average power of the sidelobes tend to decrease with increasing sampling rates.

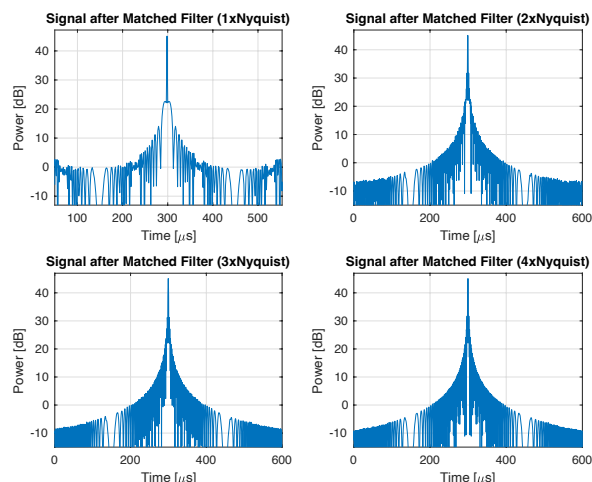


Fig. 7 - Matched filter output for different sampling rates.

In detail, this effect can be better analyzed in Fig. 8. It can be seen that the signal compression gain does not vary with increasing sample rate. This result was already expected based on (9) and the signal sampling theory. A signal discretized at rates above that stipulated by the Nyquist criterion has enough energy for its complete reconstruction, and its essential characteristics remain unchanged [13]. The same result was also acquired by [7] with the argument that the signal strength does not change with this sampling increment since the architecture of the filter spectrum is the same as the signal received by the filter.

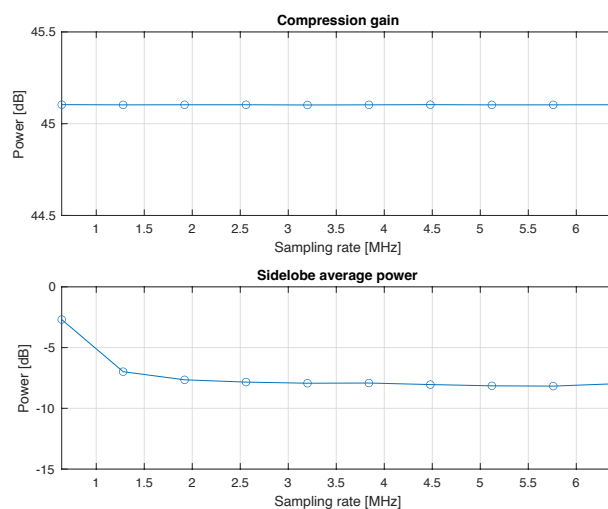


Fig. 8 - Analysis of compression gain (main lobe) and average side lobe power.

However, for values located at the lower limit of the sampling rate, an increase in the average power of the sidelobes is noticeable. This effect shows the presence of initial distortions due to undersampling [13]. In a scenario of an eventual reduction of the sampling rate below the simulated ones, it is possible to see the formation of unwanted replicas on both sides of the original pulse with a decrease in its compression gain.

C. Cross Analysis

A third round of simulations was performed, modifying both the number of bits and the signal sampling rate entering the matched filter to compare the effects of the two variables

analyzed in this paper. In this scenario, the number of bits varied from 1 to 8, and the sampling rate from 1 to 10 times the minimum frequency stipulated by Nyquist, as can be seen in Fig. 9.

About the compression gain, there is a reduction of this value with an increase of the ADC resolution up to 4 bits, as previously justified. However, there is a greater decrease of this gain between the first and second bit when the sampling rate of the signal is the one stipulated by the Nyquist criterion. There is also a slight oscillation of the compression gain when varying the sample rate in a system with resolution of up to 4 bits. After that amount, such gain does not change with an increment of sampling, an effect supported by the signal sampling theory and by (9).

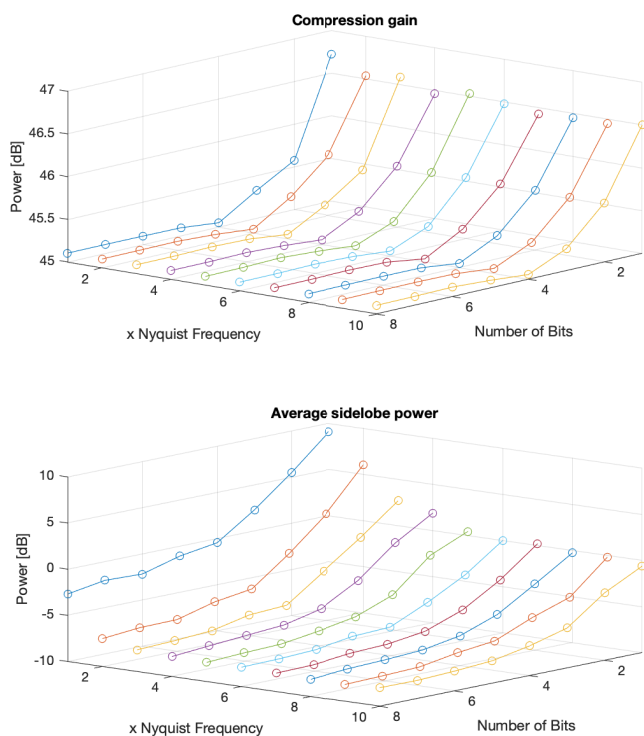


Fig. 9 – Analysis of compression gain and average sidelobe power with varying sample rates and number of bits.

Under the focus of the average sidelobe power, we notice a decrease in this value with an increase in the number of bits. This drop is more pronounced in the first 4 bits, regardless of the sampling rate. However, at rates close to Nyquist, this drop is greater. For a sampling rate at the Nyquist frequency, the average power of the sidelobes drops 9.55 dB in the first 4 bits, while for a rate ten times the Nyquist one, this reduction is 7.38 dB.

It is also possible to notice a decrease in the average sidelobe power with a sampling rate increase. However, this decrease occurs at different intensities for different bit values. For one bit, for example, such power is reduced by 9.71 dB with the variation of the sampling rate from one to ten times the Nyquist rate. But for the same range and an ADC with 8 bits, this reduction is only 5.28 dB. Therefore, depending on the processing costs in increasing the resolution or sampling, it may not be worthwhile using more complex systems since this results in minimal or no change in the sidelobe levels.

The lower graph in Fig. 9 also allows observing that there are different possible combinations of a system that deliver the same average sidelobe power. For instance, a 6-bit ADC operating at the sampling rate defined by the Nyquist criteria produces equal average sidelobe power than systems with sampling rates up to 10 times higher and low-resolution ADC.

V. CONCLUSION

In this work, we performed an analysis of the effects of varying the number of bits and the sample rate of an LFM intrapulse modulated signal on a radar receiver matched filter. We concluded that the number of bits impacts the behavior of the sidelobes and, for up to 4 bits, also affects the compression gain of the matched filter. The sampling rate, in turn, does not produce significant changes in the gain if kept within the values stipulated in the Nyquist criterion and medium to high resolution. However, for the sidelobes, rates very close to the minimum frequency cause a slight increase in the average power of these lobes. Finally, when both variables are analyzed in combination, it can be seen that if the objective is to reduce sidelobes level, different parameter values deliver same results.

ACKNOWLEDGMENTS

We gratefully thank the Brazilian Air Force, Graduation Program in Operational Applications (PPGAO), and Warfare Laboratory, ITA, for their support during the realization of this work. This study was financed in part by the Coordenação de Aperfeiçoamento de Pessoal de Nível Superior - Brasil (CAPES) - Finance Code 001

REFERENCES

- [1] M. A. Richards, J. Scheer, W. A. Holm, and W. L. Melvin, *Principles of modern radar*, vol. 1. Citeseer, 2010.
- [2] M. A. Richards, *Fundamentals of Radar Signal*. McGraw-Hill Education, 2014.
- [3] K. Davidson and J. Bray, "Understanding Digital Radio Frequency Memory Performance in Countermeasure Design," *Applied Sciences*, vol. 10, no 12, p. 4123, jun. 2020.
- [4] A. Aridgides and D. Morgan, "Effects of input quantization in floating-point digital pulse compression," *IEEE Trans Acoust*, vol. 33, no 2, p. 434–435, abr. 1985.
- [5] Hu Hang, "Study on the weighting methods of suppressing sidelobe for pulse compression of chirp signal," in *ICMMT 4th International Conference on, Proceedings Microwave and Millimeter Wave Technology, 2004.*, IEEE, p. 655–658.
- [6] J. E. Cilliers and J. C. Smit, "On the effects of quantization on mismatched pulse compression filters designed using L-p norm minimization techniques," in *IET International Conference on Radar Systems 2007*, IEE, 2007, p. 101–101.
- [7] Zhang Qunying, Yang Xuexian, and Han Yueqiu, "Effect of sampling rate on SNR in digital pulse compression system," in *ICSP '98. 1998 Fourth International Conference on Signal Processing*, IEEE, p. 23–26.
- [8] G. Turin, "An introduction to matched filters," *IEEE Trans Inf Theory*, vol. 6, no 3, p. 311–329, jun. 1960.
- [9] M. I. Skolnik, "Introduction to radar systems," *New York*, 1980.
- [10] G. Moura, "Interferência em radares de vigilância aérea: uma metodologia para análise de seus efeitos baseada na simulação e na emulação de sinais", Instituto Tecnológico de Aeronáutica, 2023.
- [11] J. B. Tsui, *Digital techniques for wideband receivers*, vol. 2. SciTech Publishing, 2004.
- [12] R. H. Walden, "Analog-to-digital converter survey and analysis," *IEEE Journal on Selected Areas in Communications*, vol. 17, no 4, p. 539–550, abr. 1999.
- [13] "Appendix A Nyquist Sampling Theorem," *Signal Processing for Cognitive Radios*, Wiley, 2014, p. 704–710.